Further investigation on the molecular dynamics in linear and multiarmed star polymers of cis-polyisoprene studied by dielectric spectroscopy*

Diethelm Boese and Friedrich Kremer
Max-Planck-Institut für Polymerforschung, Postfach 31 48, D-6500 Mainz, FRG

and Lewis J. Fetters
Exxon Research and Engineering Company, Corporate Research Laboratories, Route 22E, Annandale, NJ 08801, USA

Dielectric spectroscopy from 10^{-1} to 10^9 Hz was used to investigate bulk amorphous multiarmed stars of cis-polyisoprene and their linear counterparts, both having narrow molecular weight distributions. The star polymers resemble the linear polymers in showing two distinct regions of dielectric dispersion. A molecular weight independent segmental process occurs at nearly the same frequency as in the linear polymer. The relaxation time of the molecular weight dependent normal mode process for linear polymers can be described below a critical molecular weight M_c ($\approx 10^4$) according to the Rouse theory; but above M_c the relaxation time follows the 3.7 power of M_w, which is characteristic for entangled macromolecules. A similar dependence of the relaxation time is observed for the many arm star polymers. The arm relaxation is interpreted by means of conformational fluctuations of a tethered chain.

INTRODUCTION

Star-branched polymers with arms of equal length allow investigation of the influence of the topological structure on the molecular dynamics. In our recent studies we presented dielectric relaxation experiments on bulk linear cis-polyisoprene and multiarmed stars of polyisoprene[1,2]. Linear polymers as well as star branched polymers of cis-isoprene show two distinct regions of dielectric dispersion. Due to the lack of symmetry in its chemical structure cis-polyisoprene has non-zero components of the dipole moment both perpendicular and parallel to the chain contour. Thus two dielectric relaxation processes, a segmental and a normal mode process, are present[3–7]. The latter is caused by the parallel dipole components while the segmental mode process has its origin in local motions of the dipole components perpendicular to the chain backbone.

Experimental studies of the dielectric relaxation in star-branched molecules were started by Stockmayer and Burke[8,9]. These authors found that the dielectric relaxation time of the normal mode process in polyisoprene oxide can be predicted from the molecular weight and the bulk viscosity, using the theoretical models of Ham[10] or Zimm and Kilb[11]. Furthermore, they compared the dielectric relaxation times of linear chains with those of star-branched polymers. Adachi and Kotaka[12] discussed the degree of branching in solutions of linear poly(2,6-dichloro-1,4-phenylene oxide) and its influence on the dielectric relaxation times.

In the present paper the dielectric relaxation properties of entangled bulk amorphous 3-, 4-, 8-, 12- and 18-arm polyisoprene stars are compared with those of the linear polyisoprenes. The relaxation behaviour of the star polymers is interpreted in the framework of conformational fluctuations of a tethered chain as developed by Graessley[13].

THEORY

The complex dielectric permittivity $\varepsilon^*(\omega) = \varepsilon'(\omega) - i\varepsilon''(\omega)$ of a macroscopic system is given by the one-sided Fourier or pure imaginary Laplace transform of the time derivative of the normalized response function $\phi(t)$ for the dielectric polarization of the system[14–16]

$$\frac{\varepsilon^* - \varepsilon_\infty}{\varepsilon_{st} - \varepsilon_\infty} = \int_0^\infty \exp[-i\omega t]\left[-\frac{d\Phi(t)}{dt}\right]dt \qquad (1)$$

where ε_{st} and ε_∞ are the limiting low and high frequency permittivities respectively. The response function $\Phi(t)$ can be decomposed into contributions of dipole moment components parallel $\mu^{\parallel}$ and perpendicular $\mu^{\perp}$ to the chain contour[17]. The parallel components correspond to the end-to-end or centre-to-end distance motion:

$$\sum_j \sum_l \langle \mu_{ij}^{\parallel}(0)\mu_{il}^{\parallel}(t)\rangle = \mu^2 \langle r_i(0)r_i(t)\rangle$$

Thus $\Phi(t)$ is written as:

$$\Phi(t) = \frac{\mu^2 \langle r_i(0)r_i(t)\rangle + \sum_j \sum_l \langle \mu_{ij}^{\perp}(0)\mu_{ii}^{\perp}(t)\rangle}{\mu^2 \langle r_i(0)r_i(0)\rangle + \sum_j \sum_l \langle \mu_{ij}^{\perp}(0)\mu_{ii}^{\perp}(0)\rangle} \qquad (2)$$

where μ is a constant equal to the parallel dipole moment per unit contour length and $\langle r_i(0)r_i(t)\rangle$ is the end-to-end or centre-to-end vector autocorrelation function, respectively, for the chain i at time t. The second term of equation (2) is simply reduced to the autocorrelation function of the perpendicular dipole moment component representing segmental motions. For detailed analysis the reader should refer to References 15 and 18.

Since the relaxation times for the two components of $\Phi(t)$ are well separated in the time domain, the individual autocorrelation functions are accessible and can be calculated[17]. For non-entangled linear polymers, $\langle r_i(0)r_i(t)\rangle$ is expressed by the Rouse–Zimm theory[19,20]. According to the free draining model proposed by Rouse[19] the correlation function is given by:

$$\langle r_i(0)r_i(t)\rangle \langle r^2\rangle = (8/\pi^2) \sum (1/p^2) \exp(-t/\tau_p) \qquad (3)$$

$$\tau_p = \frac{\zeta_a N^2 b^2}{3\pi^2 k T_p^2} \qquad p = 1, 3, 5, \ldots \qquad (4)$$

where τ_p is the relaxation time for the pth normal mode, ζ_a the monomeric friction coefficient and N the number of chain segments with bond length b. Since N is proportional to the molecular weight M, the Rouse theory predicts for the longest relaxation time

$$\tau_1 \propto M^{2.0} \qquad (5)$$

For entangled polymer systems the tube model derived by de Gennes[21] predicts that the correlation function for the end-to-end vector is given by the same form as equation (3). The maximum relaxation time τ_d for the tube disengagement process is different from τ_1 defined in the Rouse theory[22]. The ratio between τ_d and τ_1 is written as

$$\tau_d/\tau_1 = 3L/b \qquad (6)$$

where L is the contour length of the primitive chain. This model predicted the $M^{3.0}$ dependence of τ_d.

The first analysis of the dynamics of non-entangled star-branched polymers was made by Ham[10] and extended in detail by Zimm and Kilb[11]. According to the free draining conditions for polymers with branches of equal length the longest relaxation time of the centre-to-end

vector of the individual arms was proposed to be:

$$\tau_2 \propto M_a^2 f^{-2} \qquad (7)$$

where f is the number of arms.

de Gennes attempted to examine the stochastic motion of highly entangled star-branched polymers[23,24]. This theory predicted that longest relaxation time of the star polymer, increases exponentially with the arm molecular weight M_a:

$$\tau_s \propto A \exp(\alpha M_a) \qquad (8)$$

having a prefactor A and a constant α. Klein[25] presented several approaches describing the dynamical quantities of star polymers and considered the diffusion and relaxation mechanisms of entangled stars in terms of the arm retraction process.

EXPERIMENTAL

The 3-, 4, 8-, 12- and 18-arm polyisoprene stars were prepared and characterized by methods described elsewhere[26-30]. Linear cis-polyisoprene was prepared by anionic polymerization in hexane at 303 K with sec-butyllithium as initiator to produce linear polymers with narrow molecular weight distributions. Weight average molecular weights (M_w) of the stars and the star arms were determined by light scattering and, in some cases for the arms, by osmotic pressure. Size exclusion chromatography (s.e.c.) was used to monitor the removal (via fractionation) of unlinked arms from the stars. For the linear cis-polyisoprene, weight-average molecular weights were determined by low-angle light scattering and osmometry while s.e.c. was used to determine the molecular weight distribution (M_w/M_n). The microstructure of linear and star-shaped cis-polyisoprene was analysed using ^{13}C-nuclear magnetic resonance[31]. The glass transition temperature T_g was determined from differential scanning calorimetry at a heating rate of 20 K min^{-1}. The results are listed in *Tables 1* and *2*.

The dielectric measurements covered the frequency range 10^{-1}–10^9 Hz. Three different measurement systems were used:

(1) a Solartron–Schlumberger frequency response analyser FRA 1254, which was supplemented by using a high-impedance preamplifier of variable gain[32], covered the frequency range from 10^{-4} to 6×10^4 Hz.

(2) In the audiofrequency range 10–10^7 Hz a Hewlett–Packard impedance analyser 4192A was used. For both

Table 1 Characteristics of linear polyisoprene

Sample[a]	$10^{-3}M_w$	M_w/M_n	T_g (K)	Microstructure, content of units (%)		
				Cis-1,4	Trans-1,4	Vinyl-3,4
PIP-01	1.1	–	200.0	74.6	18.4	7.0
PIP-05	5.1	1.03	207.1	78.8	17.9	3.3
PIP-08	8.4	1.03	211.2	78.8	16.2	5.0
PIP-13	13.1	1.03	211.5	77.9	18.1	4.0
PIP-17	17.2	1.02	213.1	76.4	17.8	5.8
PIP-38	38.2	1.03	213.1	78.6	16.7	4.7
PIP-65	65.0	1.03	213.2	78.5	16.7	4.8
PIP-97	97.0	1.02	213.2	75.7	18.1	6.2

[a] PIP-05 corresponds to polyisoprene of molecular weight 5 kg mol^{-1} etc.

Table 2 Characteristics of multiarmed polyisoprene stars

Sample[a]	$10^{-4}M_w$ (star)	$10^{-3}M_a$ (arm)	T_g (K)	Microstructure, content of units (%)		
				Cis-1,4	*Trans*-1,4	Vinyl-3,4
SPIP-3-11	3.5	11.4	213.0	78.6	16.1	5.3
SPIP-4-15	6.1	15.3	213.4	77.6	16.7	5.7
SPIP-4-30	12.2	30.5	212.2	77.6	16.8	5.6
SPIP-4-44	17.3	44.0	213.8	78.9	16.1	5.0
SPIP-4-95	38.0	95.0	213.5	77.9	16.7	5.6
SPIP-8-05	4.0	5.0	212.3	76.3	17.8	5.9
SPIP-8-08	6.0	7.5	213.6	75.4	18.5	6.1
SPIP-8-14	11.0	13.8	211.9	77.3	17.7	5.0
SPIP-8-16	12.4	15.5	213.4	80.4	15.5	4.1
SPIP-8-100	79.5	99.4	214.0	77.9	16.6	5.5
SPIP-12-03	4.1	3.4	211.7	79.1	16.6	4.3
SPIP-12-08	9.6	8.0	211.9	79.6	16.0	4.4
SPIP-12-21	25.0	20.8	212.9	80.5	15.6	3.9
SPIP-12-68	81.0	67.5	213.5	77.2	17.0	5.8
SPIP-18-03	6.4	3.5	213.1	77.4	17.4	5.2
SPIP-18-11	19.7	10.9	213.7	76.2	18.0	5.8
SPIP-18-12	21.8	12.1	212.9	77.5	17.5	5.0
SPIP-18-21	38.4	21.3	213.0	76.5	17.9	5.6
SPIP-18-44	80.0	44.4	212.5	77.2	17.2	5.6

[a] SPIP-8-05 corresponds to star polyisoprene with eight arms and an arm molecular weight of 5 kg mol^{-1} etc.

parts the sample material was kept between two condenser plates (gold plated stainless steel electrodes; diameter 40 mm).

(3) For measurements between 10^6 and 10^9 Hz Hewlett–Packard impedance analyser 4191A was used, which is based on the principle of a reflectometer. A small sample condenser (diameter 6 mm) was mounted as a part of the inner conductor of a coaxial cell.

All three arrangements were placed in custom-made cryostats wherein the sample was set in a stream of temperature-controlled nitrogen gas, which allowed temperature adjustment from 100 up to 500 K within ± 0.02 K (Reference 33).

RESULTS AND DISCUSSION

Dielectric relaxation of bulk amorphous polyisoprene stars

The temperature and frequency dependence of the dielectric loss $\varepsilon''(v)$ for bulk SPIP-8-14 (*Figure 1*) shows two distinct regions of dielectric dispersion. The two processes are well separated on the frequency and temperature scale; the initial process occurs around 220 K just above the glass transition temperature (212 K) and hence is assigned to the segmental mode process. It originates from local motions of the perpendicular dipole moment. The positions of the loss maxima arising from segmental motions are almost independent of molecular weight (*Figures 2* and *3*). In contrast, the relaxation process above 260 K exhibits a pronounced dependence on molecular weight; it shifts to higher temperature with increasing molecular weight (*Figure 2*). This trend is characteristic for a normal mode process which corresponds to motions of the entire chain caused by dipole components parallel to the chain backbone.
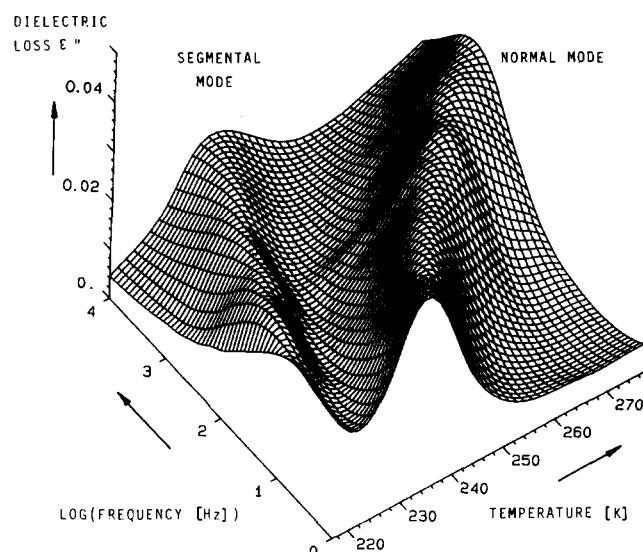

Figure 1 3D representation of the frequency and temperature dependence of the dielectric loss ε'' for the eight-arm polyisoprene star SPIP-8-14

The empirical Williams–Landel–Ferry (WLF) equation[34] was used to describe the temperature dependence of the relaxation rate v_{max} at maximum loss $\varepsilon''_{max}(v)$:

$$\log(v_{max}/v_0) = \frac{C_1(T - T_0)}{C_2 + T - T_0} \quad (9)$$

where T_0 is a reference temperature, v_0 is the corresponding relaxation rate and C_1 and C_2 are fitting parameters. The values of the parameters are calculated via a non-linear least squares fit with $T_0 = 250$ K for the segmental mode process and $T_0 = 300$ K for the normal mode process. The results are listed in *Tables 3* and *4*.

For the linear *cis*-polyisoprene the relaxation rate of the segmental mode process and hence the resulting activation parameters (*Table 3*) are almost independent of molecular weight except very low molecular weights. The same constants (*Table 4*) represent the experimental temperature dependence of the relaxation rate for the star polymers (*Figure 4*). It thus appears clear that this process reflects local motions which are independent of branching or chain length.

Attention is now directed to the normal mode process whose relaxation rates show a strong dependence on the molecular weight and demonstrate a weaker temperature dependence. In comparing linear and star polymers having nearly the same molecular weight or arm molecular weight (*Figure 4*) the following characteristics were observed[1,2]:

(1) both polymer structures exhibit the same segmental mode process;

(2) the normal mode processes for both linear and star polymers have a similar temperature dependence; but

(3) the normal mode processes of the star polymers are shifted to lower frequencies.

Correlation function for linear and star polyisoprenes

The application of equation (1) states that the complex dielectric permittivity $\varepsilon^*(\omega)$ is given by the one-sided Fourier transform of the quantity $-d\Phi(t)/dt$. Since $\varepsilon'(\omega)$ and $\varepsilon''(\omega)$ are related to each other via the Kramers–Kronig relation, further evaluation concentrates only on $\varepsilon''(\omega)$ to extract $\Phi(t)$ from the transformation of the measured quantities. This is done by a half-sided cosine
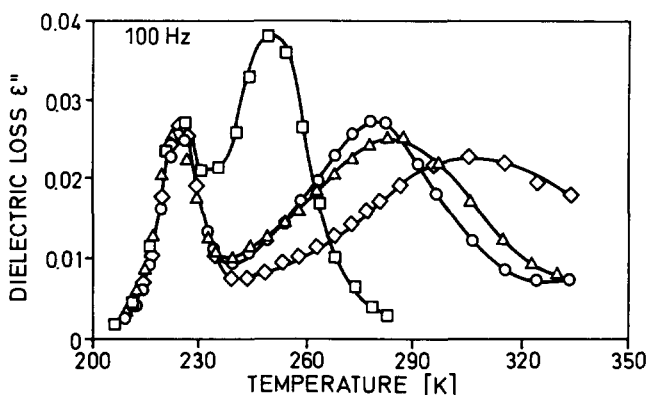

Figure 2 Temperature dependence of the dielectric loss ε'' at 100 Hz for the 18-arm polyisoprene star of different molecular weights (see *Table 2*): □, SPIP-18-03; ○, SPIP-18-11; △, SPIP-18-12; ◇, SPIP-18-21
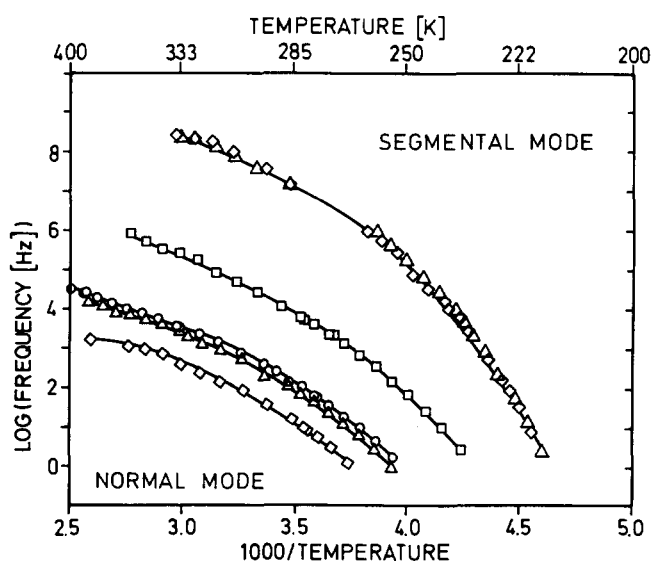

Figure 3 Activation plot for the segmental and normal mode process of the 18-arm polyisoprene star: □, SPIP-18-03; ○, SPIP-18-11; △, SPIP-18-12; ◇, SPIP-18-21
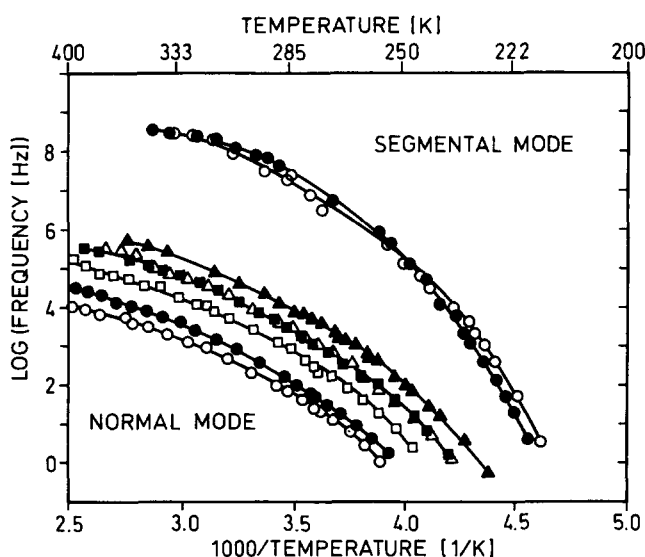

Figure 4 Activation plot for the segmental and normal mode process of the eight-arm polyisoprene (for clarity the segmental modes for SPIP-8-14 and PIP-13 only are plotted): △, SPIP-8-05; ▲, PIP-05; □, SPIP-8-08; ■, PIP-08; ○, SPIP-8-14; ●, PIP-13

Table 3 WLF parameters C_1, C_2 and v_0 determined by equation (9) for the segmental and normal mode process of linear polyisoprene

Code	Segmental mode, $T_0 = 250$ K			Normal mode, $T_0 = 300$ K		
	C_1	C_2 (K)	$10^{-5}v_0$ (Hz)	C_1	C_2 (K)	v_0 (Hz)
PIP-01				4.0	151.6	2.0×10^6
PIP-05	5.7	80.0	1.2	4.0	133.9	3.1×10^4
PIP-08	5.7	70.0	2.1	4.3	136.2	7.4×10^3
PIP-13	5.8	74.3	2.2	4.2	128.8	1.3×10^3
PIP-17	6.1	70.9	1.4	4.4	129.5	3.9×10^2
PIP-38	6.0	71.2	1.6	4.2	119.9	2.2×10^1
PIP-65	6.1	73.4	1.7	3.6	97.5	3.1
PIP-97	6.1	70.9	1.4	0.9	57.9	0.02

Table 4 WLF parameters C_1, C_2 and v_0 determined by equation (9) for the segmental and normal mode process of multiarmed polyisoprene stars

Code	Segmental mode, $T_0 = 250$ K			Normal mode, $T_0 = 300$ K		
	C_1	C_2 (K)	$10^{-5}v_0$ (Hz)	C_1	C_2 (K)	v_0 (Hz)
SPIP-3-11	6.2	75.4	1.6	3.7	111.8	3.4×10^2
SPIP-4-15	6.3	76.7	1.3	3.9	116.6	2.4×10^2
SPIP-4-30	6.2	78.7	1.3	2.3	40.0	1.6
SPIP-4-44	6.2	79.4	1.3			
SPIP-4-95	6.3	74.9	1.4			
SPIP-8-05	6.0	75.2	1.5	4.3	132.8	9.6×10^3
SPIP-8-08	6.0	72.5	1.1	4.2	127.5	2.2×10^3
SPIP-8-14	6.1	76.7	1.5	4.1	123.3	1.6×10^2
SPIP-8-16	6.3	76.6	1.4	4.0	122.4	1.3×10^2
SPIP-8-100	6.0	76.3	1.5			
SPIP-12-03	6.0	79.6	2.0	4.2	134.7	9.1×10^3
SPIP-12-08	6.1	79.8	2.0	4.0	128.8	1.8×10^3
SPIP-12-21	5.9	76.7	1.9	3.4	104.3	5.3×10^3
SPIP-12-68	6.2	73.8	1.0			
SPIP-18-03	6.3	74.9	1.3	4.7	140.8	3.1×10^4
SPIP-18-11	6.1	72.1	1.3	3.8	115.0	5.5×10^2
SPIP-18-12	6.0	72.6	1.5	3.8	114.3	3.1×10^2
SPIP-18-12	6.2	75.0	1.3	3.4	100.4	5.4×10^1
SPIP-18-44	6.2	75.1	1.3			

transformation:

$$\Phi(t) = \frac{2}{\pi} \int_0^\infty \left[\frac{\varepsilon''(\omega)}{\varepsilon_{st} - \varepsilon_\infty} \right] \frac{\cos \omega t}{\omega} \, d\omega \qquad (10)$$

Details of the calculation of $\Phi(t)$ are described elsewhere[7,35]. To the resulting correlation functions the empirical relation as given by the Kohlrausch–Williams–Watts (KWW) function

$$\Phi(t) = \exp\left[-\left(\frac{t}{\tau_{KWW}} \right)^\beta \right] \qquad 0 < \beta \leqslant 1 \qquad (11)$$

was fitted. The parameter β describes the non-exponential character of the correlation function and τ_{KWW} is the time at which $\Phi(t)$ falls to its $1/e$ point[36-38].

From the parameters determined, the mean relaxation time can be obtained via

$$\langle \tau_{KWW} \rangle = (\tau_{KWW}/\beta)\Gamma(1/\beta) \qquad (12)$$

where Γ denotes the gamma function[39].

Correlation function for the linear polyisoprenes. The parameter β for the segmental mode process is found to be constant over the entire temperature range. This holds for all samples with $8000 \leqslant M_w \leqslant 97\,000$ and reveals a molecular weight independent mean β value of 0.40 ± 0.02.

The non-exponential decay of the end-to-end vector correlation function exhibits, at temperatures where the relaxation process is far from the glass transition range, a molecular weight dependence (*Table 5*). With increasing molecular weight the parameter β decreases slightly. This behaviour was explained with the approach developed by Pakula and Geyler[40,41], who carried out computer simulations for cooperative relaxations in condensed macromolecular systems. The non-exponential decay of the end-to-end vector autocorrelation function that is observed experimentally and found in the computer simulations of Pakula and Geyler reflects mode–mode

Table 5 KWW parameters for the normal mode process at $T = 322 \pm 3$ K for linear polyisoprenes

Sample	T (K)	β	τ_{KWW} (s)	$\langle \tau_{KWW} \rangle$ (s)
PIP-08	324.4	0.65	3.0×10^{-6}	4.1×10^{-6}
PIP-13	319.9	0.61	1.9×10^{-5}	2.8×10^{-5}
PIP-17	324.4	0.61	4.5×10^{-5}	6.6×10^{-5}
PIP-38	324.4	0.54	7.5×10^{-4}	1.3×10^{-3}
PIP-65	323.8	0.54	6.0×10^{-3}	1.0×10^{-2}
PIP-97	325.1	0.52	2.0×10^{-2}	3.7×10^{-2}

interactions due to intermolecular restraints of closed packed chains.

Correlation function for the multiarmed polyisoprene stars. In comparing the 'stretched exponential' of the linear and star-branched polymers for the segmental mode process, the same temperature and arm molecular weight independent mean β value of 0.40 ± 0.01 was found. As known from dynamic mechanical measurements the terminal relaxation spectra of nearly monodisperse stars are much broader than for linear polymers and the breadth increases with arm length[42,43]. Similar behaviour is observed for the dielectric normal mode processes and a correlation between the shape parameter β and increasing arm molecular weight is only indicated for the 18-arm stars (*Table 6*). The broad dielectric loss curves and, therefore, the non-exponential decay of the end–centre vector autocorrelation function are a natural consequence of the star dynamics because the branch point prevents the simple reptation mechanism and relaxation takes place by the much slower process of contour length fluctuations: progressively larger and exponentially less frequent fluctuations are required to abandon those positions of the tube nearer the branch point[43].

Table 6 KWW parameters for the normal mode process at $T = 323 \pm 3$ K for polyisoprene stars

Sample	T (K)	β	τ_{KWW} (s)	$\langle\tau_{KWW}\rangle$ (s)
SPIP-3-11	321.7	0.46	6.5×10^{-5}	1.5×10^{-4}
SPIP-4-15	326.6	0.48	6.6×10^{-5}	1.4×10^{-4}
SPIP-8-05	319.7	0.48	3.0×10^{-6}	6.4×10^{-6}
SPIP-8-08	324.9	0.50	8.5×10^{-6}	1.7×10^{-5}
SPIP-8-14	320.1	0.48	1.3×10^{-4}	2.8×10^{-4}
SPIP-8-16	325.3	0.49	1.3×10^{-4}	2.7×10^{-4}
SPIP-12-03	325.8	0.49	2.7×10^{-6}	5.6×10^{-6}
SPIP-12-08	325.2	0.50	1.1×10^{-5}	2.2×10^{-5}
SPIP-12-21	322.4	0.47	3.8×10^{-4}	8.6×10^{-4}
SPIP-18-03	325.7	0.49	6.0×10^{-6}	1.2×10^{-7}
SPIP-18-11	324.4	0.44	2.9×10^{-5}	7.6×10^{-5}
SPIP-18-12	323.5	0.40	4.4×10^{-5}	1.5×10^{-4}
SPIP-18-21	324.3	0.38	2.5×10^{-4}	9.6×10^{-4}
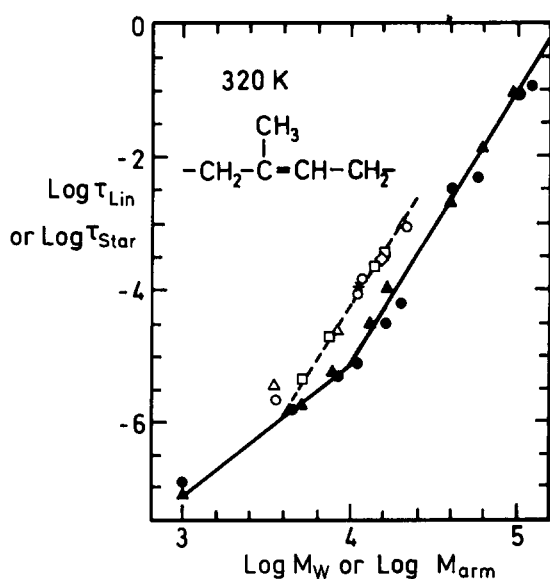
Figure 5 Dependence of the dielectric relaxation time τ on molecular weight for the normal mode process of the linear polyisoprene chain (▲) at 320 K, data reported by Adachi and Kotaka (●)[3,4], and star-branched polyisoprene: ∗, 3-arm star; ◇, 4-arm star; □, 8-arm star; △, 12-arm star; ○, 18-arm star

Molecular weight dependence of the normal mode relaxation time

The relaxation times of linear cis-polyisoprene chains and 3-, 4-, 8-, 12- and 18-arm stars calculated by using the relation $\tau = (2\pi\nu_{max})^{-1}$ at 320 K are plotted versus the molecular weight or the arm molecular weight in *Figure 5*. As reported recently[3-7], for linear cis-polyisoprene having molecular weights below the critical molecular weight M_c ($\approx 10^4$) the normal mode relaxation time was proportional to $M^{2.0}$ in agreement with the Rouse theory[19]. In the region above M_c ($\approx 10^4$) the relaxation time follows the power law with an exponent of 3.7 ± 0.1, which is characteristic of entangled polymers[22].

The dependence of the relaxation time on the arm molecular weight for various star polymers in an intermediate range from $1.0 < M_a/M_e \leqslant 4.2$ ($M_e = M_c/2$) is in close agreement ($\tau_{star} \propto M^{3.4}$) with the 3.7 power of M_w as deduced for linear chains above M_c. As seen in *Figure 5*, the relaxation times of the stars are shifted to

longer times but they are not influenced by the number of arms. Calculation of the ratio $\tau_{star}/\tau_{linear}$ for the same molecular weight or arm molecular weight reveals a mean value of 4.0 ± 0.4 (except for SPIP-8-05 and SPIP-18-03) from *Table 7*.

Graessley pointed out that the equilibration time for the conformational fluctuations of the tethered Rouse-chain would be four times that for a free linear chain of the same length[13]. Therefore, all relaxation times from *Figure 5* were divided by four and plotted in *Figure 6* versus the arm molecular weight. The result is in excellent agreement with the concept mentioned above and also proves its validity in the entanglement region. Being tethered, the chain cannot undergo a pure reptation as already deduced for star-branched polymers, but the length of its primitive path can also vary with time. Thus,

Table 7 Relaxation times of star-branched and linear polyisoprenes at $T = 320$ K

Sample	τ_{star} (s)	τ_{linear} (s)[a]	$\tau_{star}/\tau_{linear}$
SPIP-3-11	1.1×10^{-4}	2.5×10^{-5}	4.40
SPIP-4-15	2.8×10^{-4}	7.6×10^{-5}	3.72
SPIP-8-15	4.5×10^{-6}	1.9×10^{-6}	2.36
SPIP-8-08	1.9×10^{-5}	4.6×10^{-6}	4.13
SPIP-8-14	3.4×10^{-4}	8.3×10^{-5}	4.09
SPIP-8-16	2.1×10^{-4}	5.3×10^{-5}	3.96
SPIP-12-03	3.6×10^{-6}	9.5×10^{-7}	3.79
SPIP-12-08	2.2×10^{-5}	5.2×10^{-6}	4.23
SPIP-12-21	8.6×10^{-4}	2.2×10^{-4}	3.91
SPIP-18-03	2.1×10^{-6}	9.1×10^{-7}	2.30
SPIP-18-11	8.0×10^{-5}	2.1×10^{-5}	3.81
SPIP-18-12	1.4×10^{-4}	3.2×10^{-5}	4.37
SPIP-18-21	8.9×10^{-4}	2.4×10^{-4}	3.70

[a] The power laws of $M^{2.0}$ ($M_w < M_c$) and $M^{3.7}$ ($M_w \geqslant M_c$) were used to interpolate the relaxation time at a given arm molecular weight
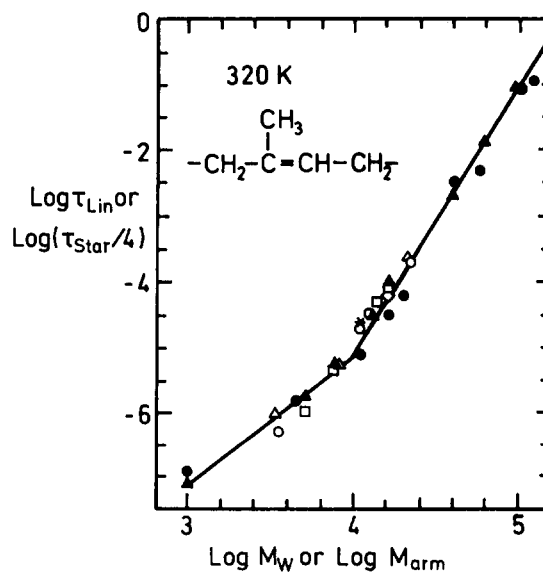
Figure 6 Dependence of the dielectric relaxation time τ on molecular weight for the normal mode process of the linear polyisoprene chain (▲) at 320 K and data reported by Adachi and Kotaka (●)[3,4]. For the star-branched polyisoprene the dielectric relaxation time $\tau_{star}/4$ is plotted versus the arm molecular weight: ∗, 3-arm star; ◇, 4-arm star; □, 8-arm star; △, 12-arm star; ○, 18-arm star

as time passes, the number of primitive segments in the path will change as Brownian motion redistributes the path and surplus populations. If the path length increases due to a momentary reduction in surplus segments the free end will move out along a random path among the obstacles, or when the path length decreases the free end will pull back, disengaging the chain from part of its previously occupied path. Such repeated breathing motions of the primitive path will result in the progressive abandonment of any initially occupied path through the surrounding obstacles, thus creating a new conformation for those parts of the fixed chain (conformational fluctuations). In effect, the initial path of a tethered chain fluctuates from the free end inwards and outwards even though pure reptation of a free linear chain is suppressed[13]. The independence of the number of arms as well as the experimentally deduced ratio of 4.0 for τ_{star} and τ_{linear} lead to the conclusion that the relaxation behaviour in star polymers can be explained by length fluctuations of a tethered chain.

CONCLUSION

We have studied the dielectric relaxation behaviour of multiarmed cis-polyisoprene stars as well as their linear counterpart in the bulk amorphous state. The molecular weight dependence of the normal mode relaxation time for linear polymers below a critical molecular weight M_c ($\approx 10^4$) obeys the Rouse theory, where τ is proportional to $M^{2.0}$. Above M_c the relaxation time is proportional to $M^{3.7}$, which is characteristic for entangled polymers. The segmental mode process for both linear and star-branched cis-polyisoprene is found to be almost independent of molecular weight and hence results in similar activation parameters and identical Kohlrausch–Williams–Watts parameters. This process is directly associated with the dynamic glass transition of the bulk polymer.

The non-exponential decay for both end-to-end and centre-to-end vector correlation function is explained by relaxation behaviour due to cooperative rearrangements. The dependence of the relaxation time on the arm molecular weight for multiarmed star isoprenes in an intermediate range $1.0 < M_a/M_c \leqslant 4.2$ is independent of the number of arms and shows close quantitative agreement with the 3.7 power as deduced for linear chains above M_c. According to Graessley, the arm relaxation time can be described by a quantitative agreement in terms of conformational fluctuations of a tethered chain.

REFERENCES

1 Boese, D., Kremer, F. and Fetters, L. J. *Makromol. Chem. Rapid Commun.* 1988, 9, 367

2 Boese, D., Kremer, F. and Fetters, L. J. *Macromolecules* 1990, 23, 1826
3 Adachi, K. and Kotaka, T. *Macromolecules* 1984, 17, 120
4 Adachi, K. and Kotaka, T. *Macromolecules* 1985, 18, 466
5 Adachi, K. and Kotaka, T. *J. Mol. Liquids* 1987, 36, 75
6 Imasishi, Y., Adachi, K. and Kotaka, T. *J. Chem. Phys.* 1988, 89, 7585
7 Boese, D. and Kremer, F. *Macromolecules* 1990, 23, 830
8 Stockmayer, W. H. *Pure Appl. Chem.* 1967, 15, 539
9 Stockmayer, W. H. and Burke, J. J. *Macromolecules* 1969, 2, 647
10 Ham, J. S. *J. Chem. Phys.* 1957, 26, 625
11 Zimm, B. H. and Kilb, R. W. *J. Polym. Sci.* 1957, 37, 19
12 Adachi, K. and Kotaka, T. *Macromolecules* 1983, 16, 1936
13 Graessley, W. W. *Adv. Polym. Sci.* 1982, 47, 67
14 Nee, T.-H. and Zwanzig, R. *J. Chem. Phys.* 1970, 52, 6353
15 Williams, G. *Chem. Soc. Rev.* 1972, 72, 55
16 Williams, G. *Chem. Soc. Rev.* 1977, 7, 89
17 Adachi, K. and Kotaka, T. *Macromolecules* 1988, 21, 157
18 Williams, G., Cook, M. and Hains, P. J. *J. Chem. Soc. Faraday Trans. II* 1972, 68, 1045
19 Rouse, P. E. *J. Chem. Phys.* 1953, 21, 1272
20 Zimm, B. H. *J. Chem. Phys.* 1956, 24, 269
21 de Gennes, P. G. *J. Chem. Phys.* 1971, 55, 572
22 Doi, M. and Edwards, S. F. 'The Theory of Polymer Dynamics', Clarendon Press, Oxford, 1988
23 de Gennes, P. G. *J. Phys. Paris* 1975, 36, 1199
24 de Gennes, P. G. 'Scaling Concepts in Polymer Physics', Cornell University Press, New York, 1979
25 Klein, J. *Macromolecules* 1986, 19, 105
26 Morton, M. and Fetters, L. J. *Rubber Chem. Technol.* 1975, 48, 359
27 Hadjichristidis, N., Guyot, A. and Fetters, L. J. *Macromolecules* 1978, 11, 668
28 Hadjichristidis, N. and Fetters, L. J. *Macromolecules* 1980, 13, 191
29 Kow, C., Morton, M., Fetters, L. J. and Hadjichristidis, N. *Rubber Chem. Technol.* 1982, 55, 245
30 Bauer, B. J., Fetters, L. J., Graessley, W. W., Hadjichristidis, N. and Quack, G. F. *Macromolecules* 1989, 22, 2237
31 Sato, H., Ono, A. and Tanaka, Y. *Polymer* 1977, 18, 580
32 Pugh, J. and Ryan, J. T. IEE Conference on Dielectric Materials, Measurements and Applications, London, Vol. 144, 1979, p. 404
33 Kremer, F., Boese, D., Meier, G. and Fischer, E. W. *Prog. Coll. Polym. Sci.* 1989, 80, 129
34 Ferry, J. D. 'Viscoelastic Properties of Polymers', 3rd Edn., Wiley, New York, 1980
35 Boese, D., Momper, B., Meier, G., Kremer, F., Hagenah, J.-U. and Fischer, E. W. *Macromolecules* 1989, 22, 4416
36 Williams, G. and Watts, D. C. *Trans. Faraday Soc.* 1970, 66, 80
37 Cook, M., Watts, D. C. and Williams, G. *Trans. Faraday Soc.* 1970, 66, 2503
38 Williams, G., Watts, D. C., Dev, S. B. and North, A. M. *Trans. Faraday Soc.* 1971, 67, 1323
39 Lindsay, C. D. and Patterson, G. D. *J. Chem. Phys.* 1980, 73, 3348
40 Pakula, T. and Geyler, S. *Macromolecules* 1987, 20, 2909
41 Pakula, T. and Geyler, S. 'Polymer Motion in Dense Systems' (Eds. D. Richter and T. Springer), Springer-Verlag, Berlin, 1988
42 Pearson, D. S., Mueller, S. J., Fetters, L. J. and Hadjichristidis, N. *J. Polym. Sci., Polym. Phys. Edn.* 1983, 21, 2287
43 Graessley, W. W. 'Molecular Conformation and Dynamics of Macromolecules in Condensed Systems' (Ed. M. Nagasawa), Elsevier, New York, 1988